Supporting Information for:

Sulfur versus Iron Oxidation in an Iron-Thiolate Model Complex

Aidan R. McDonald,[a] Michael R. Bukowski,[a,e] Erik R. Farquhar,[a] Timothy A. Jackson,[a,f] Kevin D. Koehntop,[a] Mi Sook Seo,[b] Raymond F. De Hont,[c] Audria Stubna,[c] Jason A. Halfen,[d] Eckard Münck,[c,] Wonwoo Nam,[b,]* and Lawrence Que, Jr.[a,]**

Department of Chemistry and Center for Metals in Biocatalysis, 207 Pleasant Street S.E., University of Minnesota, Minneapolis, MN 55455; Department of Bioinspired Science, Department of Chemistry and Nano Science, Center for Biomimetic Systems, Ewha Womans University, Seoul 120-750, Korea;; Department of Chemistry, Carnegie Mellon University, Mellon Institute, 4400 Fifth Ave., Pittsburgh, PA 15213, and Department of Chemistry, University of Wisconsin-Eau Claire, 443 Phillips Hall, Eau Claire, WI 54702

larryque@umn.edu , wwnam@ewha.ac.kr , emunck@cmu.edu

RECEIVED DATE

[a] University of Minnesota

[b] Ewha Womans University

[c] Carnegie Mellon University

[d] University of Wisconsin-Eau Claire

[e] Current address: Department of Chemistry, Penn State Altoona, Altoona, PA 1660

[f] Department of Chemistry, University of Kansas, Lawrence, KS 66045

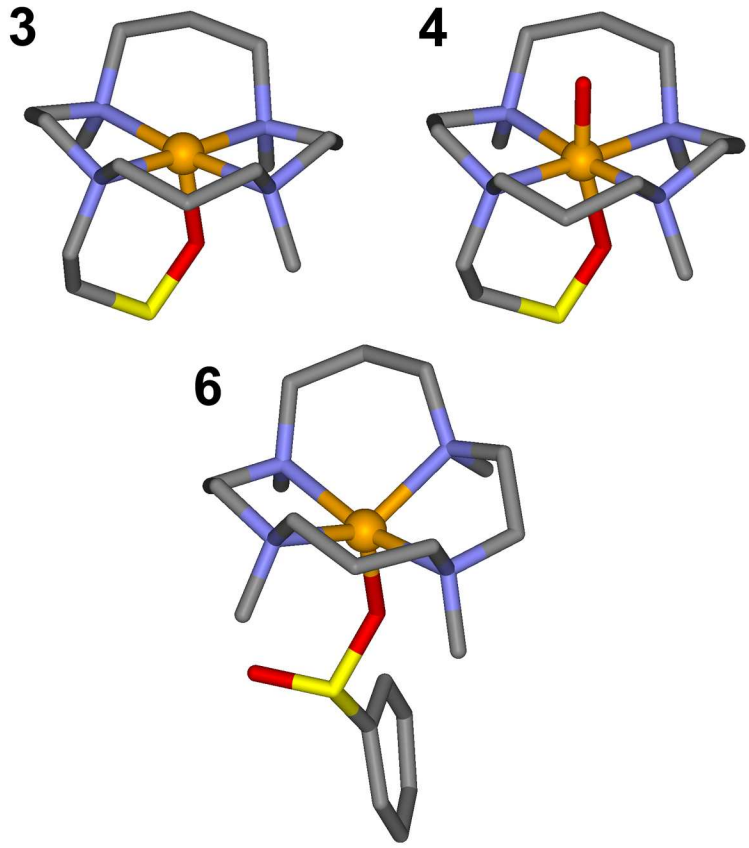

Figure S1. FEFF input models for **3**, **4**, and **6**. The structures were generated using ChemBio 3D Ultra 11.0 (Cambridgesoft) and Accelrys DS Visualizer 1.7 (Accelrys Software Inc.). The central iron atom is shown as an orange sphere, while other atoms are shown as sticks (carbon = grey, nitrogen = blue, oxygen = red, sulfur = yellow).

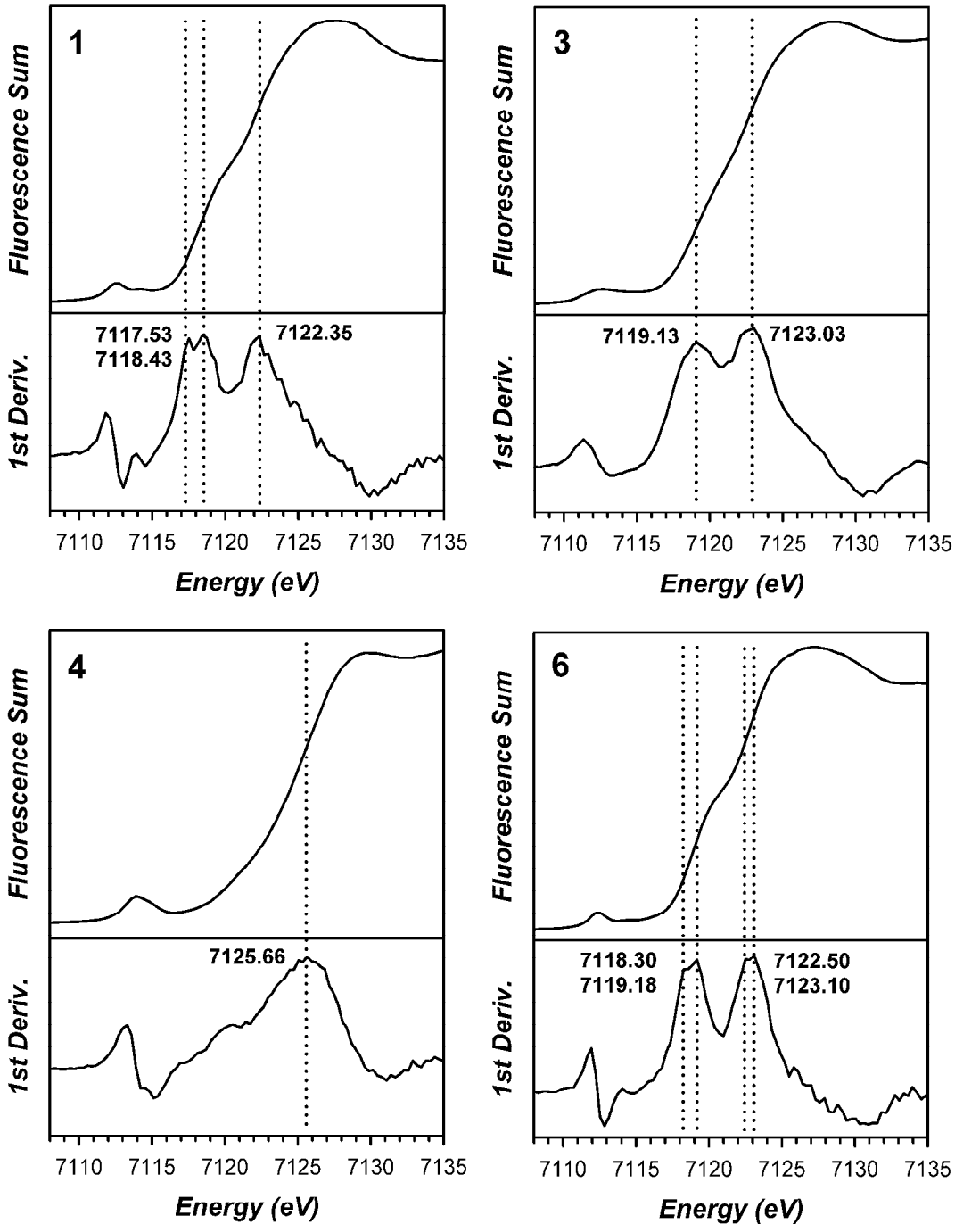

Figure S2. Fe K-edge XANES spectra and first derivatives thereof for **1** (upper left), **3** (upper right), **4** (lower left), and **6** (lower right). The dotted lines indicate the position of maxima in the first derivative associated with inflection points in the XANES spectra, with energies shown in bold-face.

Table S1. Pre-edge analysis parameters for **1**, **3**, **4**, and **6**. Values in parentheses represent uncertainties in the respective parameters.[a]

Species	E_{edge} *(eV)*	$E_{preedge}$ *(eV)*	*height*	*width*	*area*
1	7122.35	7112.52(3) 7114.35(6)	0.069(1) 0.027(2)	1.86(7) 1.25(12)	13.6(5) 3.6(5)
3[b,c]	7123.03	7112.59(2)	0.043(2)	2.93(9)	13.4(9)
4[b]	7125.66	7114.08(1)	0.0932(7)	2.508(23)	24.9(2)
6	7123.10	7112.36(1) 7114.25(7)	0.0550(9) 0.0098(8)	1.42(3) 1.44(19)	8.3(2) 1.5(2)

[a] The fits presented are those that give the best agreement to the experimental data and its second derivative.
[b] The XAS sample of **3** was shown by Mössbauer analysis to contain 75% **3**, 11% **4**, and 14% of an unidentified Fe(III) species. The XAS sample of **4** was 80% in **4**, based on UV/Vis spectroscopy. The peak areas given have not been weighted for the purity of the respective samples.
[c] There is evidence for a very weak shoulder in the pre-edge feature of **3**. However we were not able to accurately model this shoulder peak with our analysis protocol. The lower resolution and broadening of the pre-edge of **3** can be attributed to the lower resolution of the Si(111) crystal monochromator at NSLS X9B compared to the Si(220) crystal monochromator used at SSRL 7-3 for collecting the XAS data on **1**, **4**, and **6**.

Table S2. EXAFS Fitting Results for **1**.[a]

	Fe-N/O			Fe-S			Fe•••C			
fit	n	*r*	σ^2	n	*r*	σ^2	n	*r*	σ^2	F [b]
1	4	2.19	0.7							0.480
2	5	2.18	1.6							0.506
3	6	2.18	2.6							0.558
4	4	2.19	2.2	1	2.29	2.6				0.436
5	5	2.20	2.6	1	2.27	2.6				0.446
6				1	2.27	-0.6				0.572
7	4	2.19	2.3	1	2.29	2.4				0.436
8	5	2.20	3.5	1	2.28	1.6				0.445
9	4	2.19	2.1	1	2.29	2.6	3	3.07	7.5	0.396
10	4	2.19	2.1	1	2.29	2.6	4	3.07	8.5	0.391
11	*4*	*2.19*	*2.1*	*1*	*2.29*	*2.7*	*5*	*3.07*	*9.7*	*0.389*
12	4	2.19	2.3	1	2.29	2.4	6	3.06	10.8	0.390
13	4	2.19	2.4	1	2.29	2.3	7	3.06	11.9	0.393
14	4	2.19	2.0	1	2.28	2.3	3 3	2.99 3.14	0.9 -0.0	0.355
15	4	2.19	2.2	1	2.28	2.0	3 4	2.98 3.13	0.8 1.3	0.360
16	*4*	*2.19*	*2.0*	*1*	*2.28*	*2.7*	*4* *4*	*2.98* *3.14*	*2.1* *1.2*	*0.366*
17	4	2.19	2.0	1	2.28	2.5	4 5	2.97 3.13	2.0 2.3	0.375
18	4	2.19	2.7	1	2.29	2.0	5 4	3.07 3.55	9.8 6.4	0.357
19	*4*	*2.19*	*2.6*	*1*	*2.29*	*2.0*	*5* *6*	*3.07* *3.55*	*9.9* *8.4*	*0.354*
20	4	2.19	2.6	1	2.29	2.0	5 8	3.08 3.56	9.7 10.7	0.356
21	4	2.19	2.4	1	2.29	1.9	4 4 4	2.99 3.15 3.54	2.1 0.9 5.5	0.320
22	***4***	***2.19***	***2.2***	***1***	***2.29***	***2.2***	***4*** ***4*** ***6***	***2.99*** ***3.16*** ***3.54***	***2.3*** ***1.0*** ***8.1***	***0.312***
23	4	2.19	2.3	1	2.29	2.0	4 4 8	2.99 3.15 3.54	2.5 1.1 11.1	0.310

[a] Fourier transform range k = 2.0 – 15.0 Å^{-1} (resolution = 0.121 Å). r is in units of Å; σ^2 is in units of 10^{-3} Å^2. All fits are to unfiltered data.

[b] Goodness-of-fit parameter F defined as $[\Sigma k^6(\chi_{exptl}-\chi_{calc})^2 / \Sigma k^6 \chi_{exptl}^2]^{1/2}$.

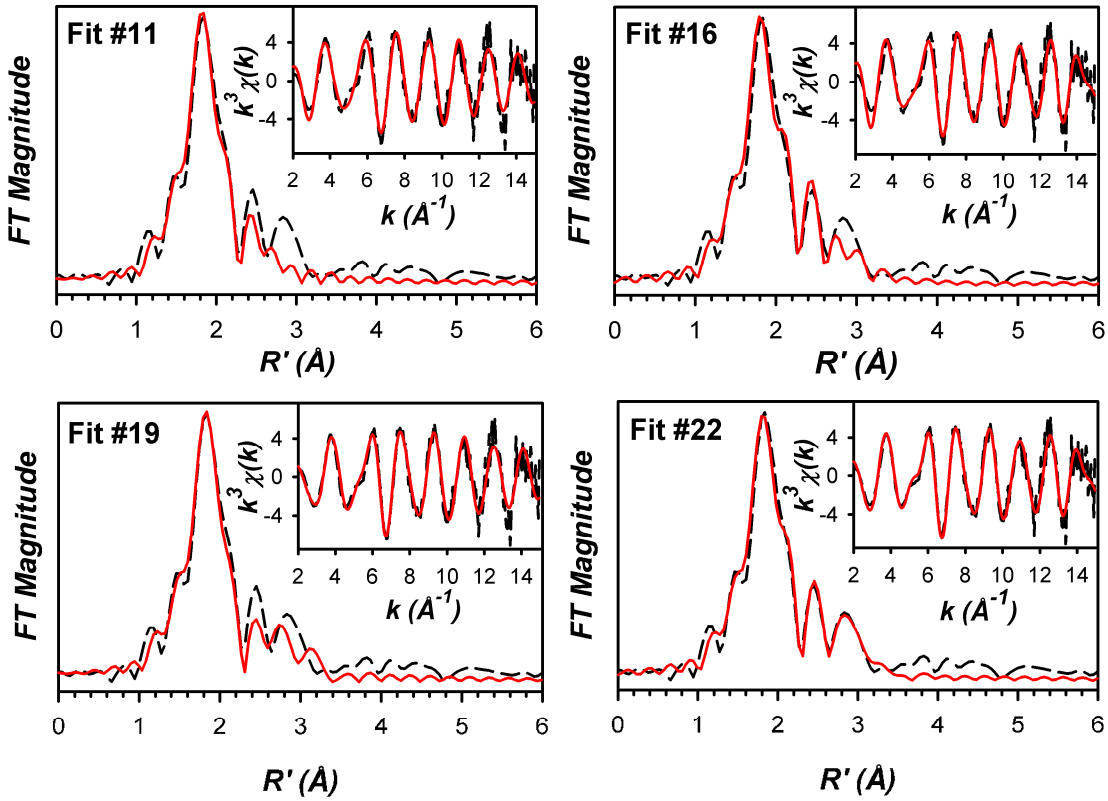

Figure S3. Fits to the Fourier transforms of the Fe K-edge EXAFS data ($k^3\chi(k)$) and unfiltered EXAFS spectra ($k^3\chi(k)$, inset) for **1**. Experimental data is shown with dashed lines (- - - -), while fits are shown with solid red lines (——). Fourier transformation range: $k = 2 – 15$ Å^{-1}. Fit parameters associated with the stated fit are shown in Table S2.

EXAFS analysis of an acetonitrile solution of **1** (Table S2, Figure S3) shows that the structure determined by x-ray crystallography is retained in solution. The inner shell can be modeled by 4 Fe–N scatterers at 2.19 Å (crystallographic Fe–N_{ave} = 2.20 Å) and 1 Fe–S at 2.29 Å (crystallographic Fe–S = 2.296 Å), and the two shells may be added in either order. A relatively simple outer-shell fit (fit #11, Table S2) with a single Fe•••C shell at 3.07 Å affords an excessively high σ^2 value of 9.7×10^{-3} Å^{-2} and a comparatively poor fit to the $k^3\chi(k)$ data and its Fourier transform (Figure S3). More elaborate fits showed that the best visual fit to the data requires three shells of Fe•••C scatterers at 2.99 Å, 3.16 Å, and 3.54 Å (fit #22, Table S2 and Figure S3); this fit accurately reproduces the bump at $k \sim 5$ Å^{-1} in the $k^3\chi(k)$ data. The additional fit complexity can be justified by the significant improvement in F to 0.312 for the five-shell fit #22 compared with F = 0.389 for the simpler three-shell fit #11.

Table S3. EXAFS Fitting Results for **3**.[a]

	Fe-N/O			Fe-O/N			Fe•••S			Fe•••C			
fit	n	*r*	σ^2	n	*r*	σ^2	n	*r*	σ^2	n	*r*	σ^2	F [b]
1	3	2.21	5.1										0.722
2	4	2.21	11.8										0.754
3	5	2.22	24.5										0.770
4	6	2.22	32.3										0.786
5	3	2.19	3.1	1	1.97	1.1							0.582
6	3	2.20	2.2	2	1.98	6.4							0.615
7	4	2.19	5.8	1	1.95	0.7							0.605
8	5	2.19	8.7	1	1.94	0.6							0.646
9	*3*	*2.19*	*3.3*	*1*	*1.96*	*1.2*	*1*	*3.27*	*5.5*				*0.507*
10	3	2.18	3.5	1	1.95	0.9	1	3.26	3.0	3	2.97	2.9	0.376
11	***3***	***2.18***	***3.5***	***1***	***1.95***	***0.8***	***1***	***3.27***	***2.9***	***4***	***2.97***	***4.6***	***0.378***
12	3	2.18	3.4	1	1.95	0.7	1	3.27	2.9	5	2.97	6.2	0.390
13	3	2.18	3.2	1	1.96	0.7				3	2.99	5.7	0.474
14	3	2.18	3.1	1	1.96	0.6				4	3.00	7.7	0.463
15	*3*	*2.18*	*3.2*	*1*	*1.96*	*0.6*				*5*	*3.00*	*9.5*	*0.459*
16	3	2.18	3.2	1	1.96	0.5				6	3.00	11.0	0.462
18	3	2.18	3.5	1	1.95	0.8	1	3.27	2.9	4	2.97	4.6	0.379
19							1	3.27	3.3				0.947
20	3	2.21	5.3				1	3.29	3.6				0.663
21	3	2.19	3.2	1	1.96	1.2	1	3.26	5.3				0.506
22	3	2.18	3.5	1	1.95	0.8	1	3.27	2.8	4	2.97	4.6	0.379

[a] Fourier transform range k = 2.0 – 14.0 Å^{-1} (resolution = 0.131 Å). r is in units of Å; σ^2 is in units of 10^{-3} Å^2. All fits are to unfiltered data.

[b] Goodness-of-fit parameter F defined as $[\Sigma k^6(\chi_{exptl}-\chi_{calc})^2 / \Sigma k^6 \chi_{exptl}^2]^{1/2}$.

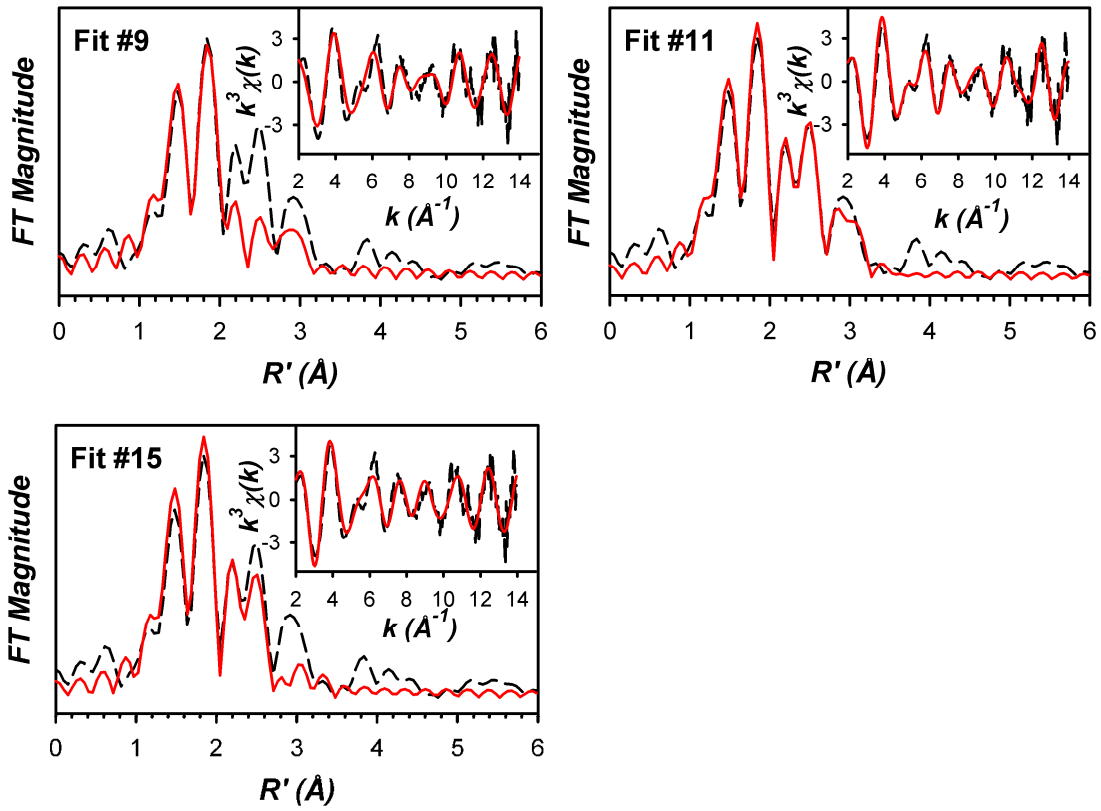

Figure S4. Fits to the Fourier transforms of the Fe K-edge EXAFS data ($k^3\chi(k)$) and unfiltered EXAFS spectra ($k^3\chi(k)$, inset) for **3**. Experimental data is shown with dashed lines (**- - - -**), while fits are shown with solid red lines (——). Fourier transformation range: $k = 2 - 14$ Å^{-1}. Fit parameters associated with the stated fit are shown in Table S3.

EXAFS analysis of a methanolic solution of **3** (Table S3, Figure S4) is consistent with an O-bound sulfinate moiety. Modeling the inner shell as a single shell of Fe–N scatterers at 2.22 Å affords exceptionally large σ^2 values, thus suggesting that this shell may be split. Indeed, a split first shell containing 3 Fe–N at 2.19 Å and 1 Fe–O at 1.97 Å provides a significant improvement in goodness of fit. The Fe–N bond length is consistent with the high-spin Fe(II) formulation obtained from Mössbauer analysis. The coordination number of the principal Fe–N shell is underestimated, which we attribute to the intrinsic 20-25% error in coordination numbers determined via EXAFS analysis, as well as heterogeneity in the sample of **3** examined here (75% **3**, 11% **4**, and 14% of an unidentified Fe(III) species, based on Mössbauer analysis), in that the contaminants presumably destructively interfere with EXAFS features arising from **3**. The outer shell can be modeled with 4 Fe•••C scatterers at 2.97 Å and 1 Fe•••S scatterer at 3.27 Å (fit #11, Table S3, Figure S4). These shells can be added in either order and indeed the fit can start with the Fe•••S shell (fits #19 – 22), suggesting that the best fit is a global minimum within the constraints of our EXAFS analysis.

Table S4. EXAFS Fitting Results for **4**.

	Fe-N/O			Fe-O/N			Fe•••C			
fit	n	*r*	σ^2	n	*r*	σ^2	n	*r*	σ^2	F [b]
1	3	2.07	2.4							0.562
2	4	2.07	3.8							0.529
3	5	2.07	5.1							0.531
4	6	2.06	6.4							0.559
5	4	2.07	3.9	1	1.64	4.0				0.466
6	4	2.07	3.8	0.8	1.64	2.6				0.447
7	5	2.06	5.3	1	1.64	4.2				0.443
8	*5*	*2.06*	*5.2*	*0.8*	*1.64*	*2.7*				*0.430*
9	*4*	*2.08*	*2.6*	*0.8* *1*	*1.640* *1.934*	*3.60* *1.98*				*0.423*
10	3	2.09	0.7	0.8 1	1.633 1.957	3.92 -0.30				0.435
11	3	2.08	2.7	0.8 2	1.639 1.974	3.06 7.08				0.428
12	4	2.08	1.8	1	1.94	0.0				0.519
13	4	2.09	3.3	2	1.96	4.8				0.570
14	3	2.09	0.0	1	1.95	-1.4				0.499
15	3	2.10	1.2	2	1.97	2.4				0.529
16	5	2.06	5.2	0.8	1.64	2.6	3	2.96	7.5	0.407
17	***5***	***2.06***	***5.2***	***0.8***	***1.64***	***2.7***	***4***	***2.96***	***9.3***	***0.411***
18	5	2.06	5.1	0.8	1.64	2.6	5	2.96	11.3	0.419
19	5	2.06	5.1	0.8	1.64	2.6	2 3	2.87 3.01	1.7 2.4	0.407
20	5	2.06	5.1	0.8	1.64	2.5	2 2	2.88 3.02	1.2 0.1	0.399
21	5	2.06	5.2	0.8	1.63	2.6	2 4	2.85 3.00	1.5 3.6	0.418
22	5	2.06	5.2	0.8	1.63	2.6	3 3	2.87 3.02	3.9 2.5	0.417
23	*5*	*2.06*	*5.2*	*0.8*	*1.64*	*2.7*	*4* *4*	*2.98* *3.42*	*9.5* *6.4*	*0.381*
24	5	2.06	5.2	0.8	1.64	2.7	4 5	2.98 3.42	9.4 8.7	0.381
25	5	2.06	5.2	0.8	1.64	2.7	4 3	2.97 3.42	9.4 4.6	0.382

[a] Fourier transform range k = 2.0 – 14.95 Å^{-1} (resolution = 0.121 Å). r is in units of Å; σ^2 is in units of 10^{-3} Å^2. All fits are to unfiltered data.

[b] Goodness-of-fit parameter F defined as $[\Sigma k^6(\chi_{exptl}-\chi_{calc})^2 / \Sigma k^6 \chi_{exptl}^2]^{1/2}$.

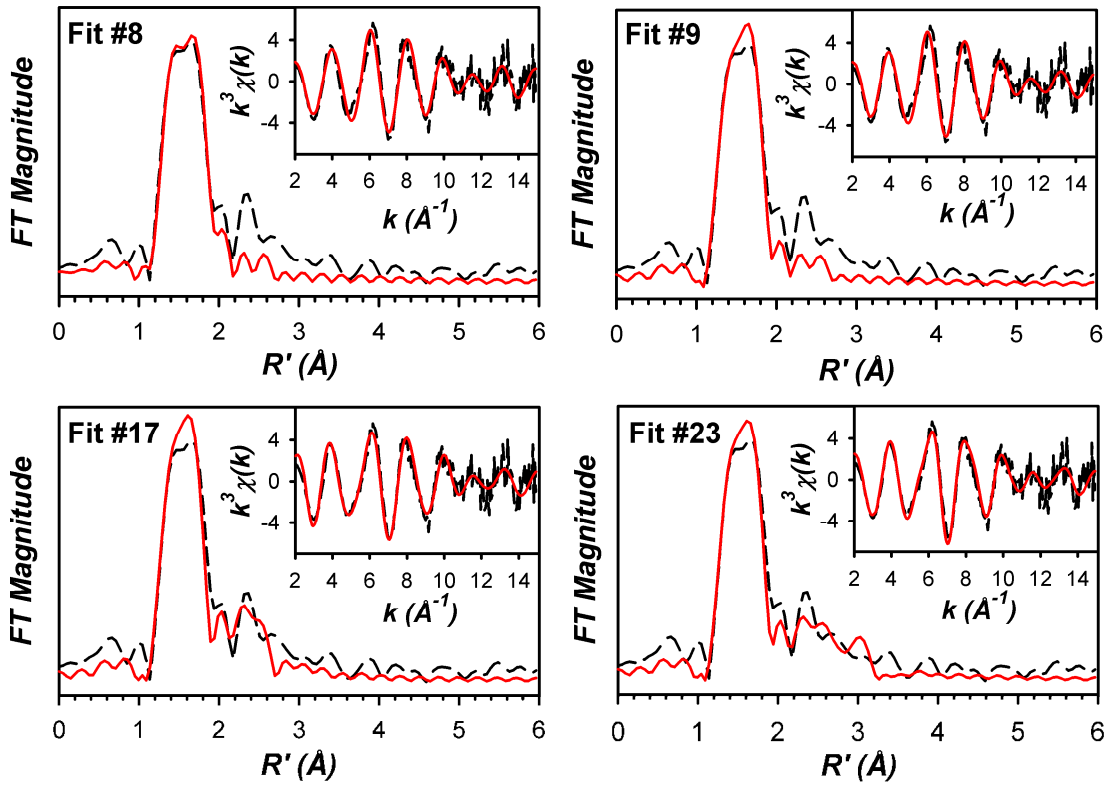

Figure S5. Fits to the Fourier transforms of the Fe K-edge EXAFS data ($k^3\chi(k)$) and unfiltered EXAFS spectra ($k^3\chi(k)$, inset) for **4**. Experimental data is shown with dashed lines (**- - - -**), while fits are shown with solid red lines (——). Fourier transformation range: $k = 2 – 14.95$ Å^{-1}. Fit parameters associated with the stated fit are shown in Table S4.

The EXAFS spectra obtained for **4** exhibit a significant attenuation in $k^3\chi(k)$ amplitude for $k > 10$ Å^{-1}, in contrast to the data obtained for **1**, **3**, and **6**. Similarly, the outer-shell features in the Fourier transform are comparatively weak. The inner shell can be fit to 5 Fe–N at 2.06 Å and 0.8 Fe=O at 1.64 Å (fit #8, Table S4 and Figure S5). A coordination number of 0.8 for the Fe=O shell was employed to better reflect the measured sample purity of 80% in **4**, as possible impurities were not expected to exhibit such a short scatterer. Consistent with this notion, fits with 0.8 Fe=O exhibit improved fit quality and Debye-Waller factors compared to those with 1.0 Fe=O (compare fits # 5 – 8). The Fe–N bond length is *ca.* 0.15 Å shorter than that of 1 and 3, consistent with oxidation of a high-spin Fe(II) center to low-spin Fe(IV), while the Fe=O bond length is similar to that of other Fe(IV)(O)(TMC)(X) complexes. It was possible to split the primary Fe–N shell into a shell of 3 – 4 Fe–N at 2.08 Å and 1 Fe–O at *ca.* 1.96 Å (fits #9 – 15). However, the difference in bond lengths is nearly identical to the resolution of the data (0.122 Å) and the magnitude of F is unchanged relative to fit #8, suggesting that this split shell cannot be justified by the available data. Indeed, the $k^3\chi(k)$ EXAFS modulations are largely accounted for by these two shells, as addition of outer shell Fe•••C scatterers generally resulted in extremely small improvements in F. There is no evidence for an Fe•••S scatterer in the EXAFS, and we thus conclude that while the EXAFS provides convincing evidence for an Fe=O interaction, it does not provide any insight into the nature of the axial ligation *trans* to the oxo.

Table S5. EXAFS Fitting Results for **6**.

	Fe-N/O			Fe-O/N			Fe•••S			Fe•••C			
fit	n	*r*	σ^2	n	*r*	σ^2	n	*r*	σ^2	n	*r*	σ^2	F [b]
1	3	2.22	2.9										0.650
2	4	2.21	5.6										0.680
3	5	2.20	10.4										0.717
4	6	2.19	17.4										0.740
5	3	2.21	2.0	1	1.99	4.0							0.598
6	4	2.20	4.2	1	1.96	2.3							0.593
7	5	2.19	6.4	1	1.95	1.5							0.609
8	*4*	*2.20*	*4.4*	*1*	*1.96*	*1.9*	*1*	*3.29*	*1.4*				*0.492*
9	4	2.18	4.5	1	1.95	1.3	1	3.28	0.9	3	2.98	2.7	0.400
10	***4***	***2.18***	***4.5***	***1***	***1.95***	***1.3***	***1***	***3.28***	***0.7***	***4***	***2.99***	***4.3***	***0.402***
11	4	2.18	4.5	1	1.95	1.3	1	3.28	0.7	5	2.99	6.1	0.410
12	4	2.19	4.3	1	1.96	1.9				3	3.04	9.3	0.533
13	4	2.19	4.3	1	1.96	1.9				4	3.04	10.5	0.524
14	*4*	*2.19*	*4.3*	*1*	*1.96*	*2.0*				*5*	*3.04*	*11.8*	*0.521*
15	4	2.19	4.3	1	1.96	2.1				6	3.04	13.0	0.523
17	4	2.18	4.5	1	1.95	1.3	1	3.28	0.8	4	2.99	4.3	0.402
18							1	3.28	1.5				0.932
19							1	3.27	1.0	4	2.97	4.3	0.846
20	4	2.21	5.9				1	3.30	1.8				0.603
21	1	2.20	4.4	1	1.96	1.9	1	3.29	1.4				0.492
22	4	2.18	4.5	1	1.95	1.3	1	3.28	0.7	4	2.99	4.4	0.402
23	*4*	*2.18*	*4.7*	*1*	*1.95*	*1.7*				*4* *4*	*2.98* *3.16*	*1.6* *1.4*	*0.467*
24	4	2.18	4.6	1	1.95	1.6				4 2	3.00 3.17	2.8 -1.6	0.445
25	4	2.18	4.7	1	1.95	1.7				4 6	2.97 3.14	0.1 2.2	0.461

[a] Fourier transform range k = 2.0 – 14.3 Å^{-1} (resolution = 0.128 Å). r is in units of Å; σ^2 is in units of 10^{-3} Å^2. All fits are to unfiltered data.

[b] Goodness-of-fit parameter F defined as $[\Sigma k^6(\chi_{exptl}-\chi_{calc})^2 / \Sigma k^6 \chi_{exptl}^2]^{1/2}$.

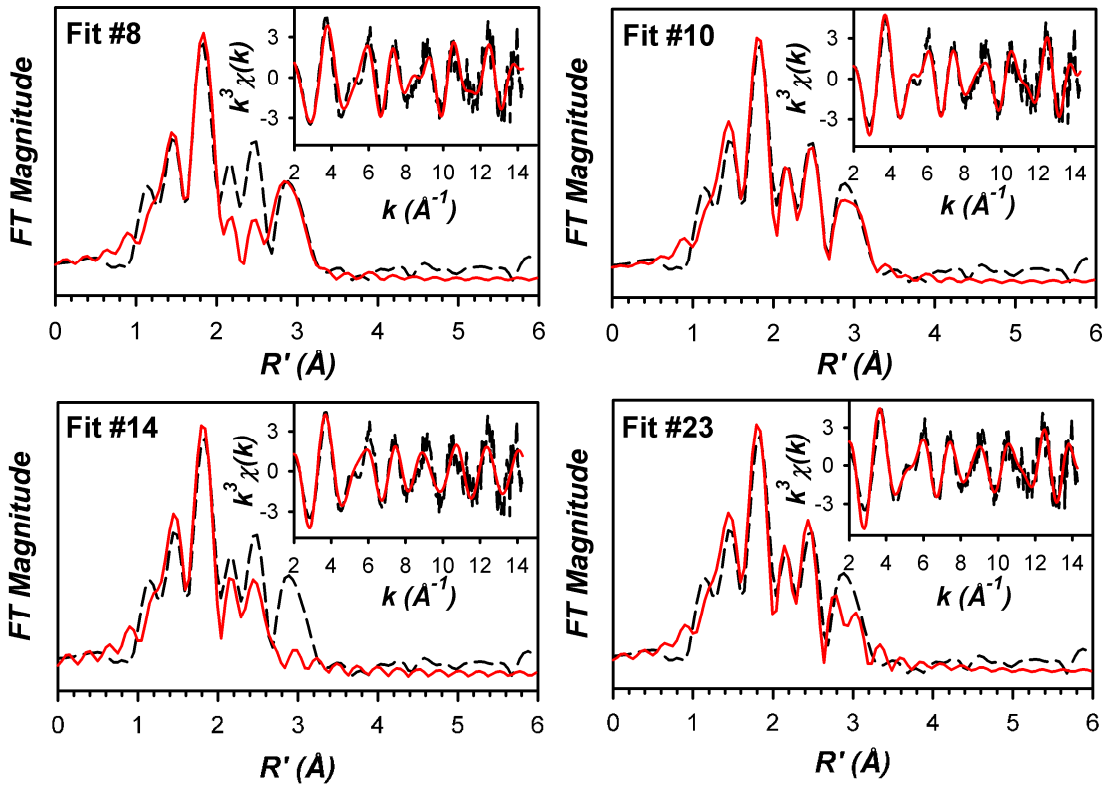

Figure S6. Fits to the Fourier transforms of the Fe K-edge EXAFS data ($k^3\chi(k)$) and unfiltered EXAFS spectra ($k^3\chi(k)$, inset) for **6**. Experimental data is shown with dashed lines (**- - - -**), while fits are shown with solid red lines (——). Fourier transformation range: $k = 2 – 14.3$ Å^{-1}. Fit parameters associated with the stated fit are shown in Table S5.

EXAFS analysis of a THF solution of **6** (Table S5, Figure S6) shows that the structure of **6** determined by x-ray crystallography is retained in solution, with some caveats. Much as was the case for **3**, modeling the inner shell as a single shell of Fe–N scatterers at 2.20 Å affords large σ^2 values, thus suggesting that this shell may be split. A split first shell (fit #6, Table S5) consisting of 4 Fe—N at 2.20 Å (crystallographic Fe–N_{ave} = 2.21 Å) and 1 Fe–O at 1.96 Å (crystallographic Fe–O = 1.995 Å) leads to significantly improved σ^2 and goodness-of-fit values. The outer shell can be modeled with 4 Fe•••C scatterers at 2.99 Å and 1 Fe•••S at 3.28 Å (fit #10, Table S5, Figure S6). As in the case of **3**, these shells may be added in either order, and the overall EXAFS fit can start from the Fe•••S shell. Finally, we note that attempting to fit the data to two shells of Fe•••C scatterers at *ca.* 3.00 Å and 3.17 Å (fit #23, Table S5, Figure S6) results in a poorer fit to the data relative to an Fe•••C/Fe•••S combination. These observations, coupled to the known x-ray crystal structure of **6**, lend further support to our proposed structural model for **3** (*i.e.*, Fe•••C scatterers can be uniquely associated with the shell at 3.0 Å, while the shell at 3.28 Å is distinctly that of Fe•••S).

We note that the EXAFS analysis of **6** indicates that the Fe–$O_{sulfinate}$ bond length is somewhat shorter in solution (1.95 Å in solution versus 1.995 Å in the crystal structure), while the Fe•••S distance lengthens significantly (3.28 Å in solution versus 3.175 Å in the crystal structure). The

refined EXAFS distances were initially arrived at using phase and amplitude parameters calculated using the crystal structure coordinates of **6** as a FEFF input model. The input model was subsequently adjusted to account for the Fe–$O_{sulfinate}$ and Fe•••S distances from EXAFS, and the EXAFS analysis redone using this refined model (the fits presented in Table S5 are for the refined model). However, there was no difference in the distances obtained, thus illustrating two points. First, phase and amplitude parameters at the single scattering level of theory are not especially sensitive to distance differences of less than 0.1 Å. Secondly, there is some modest change in the structure of the Fe–sulfinate moiety in this complex in THF solution relative to the crystal structure (obtained from a CH_2Cl_2 solution). At the moment, we are unable to offer a rational explanation for this difference.

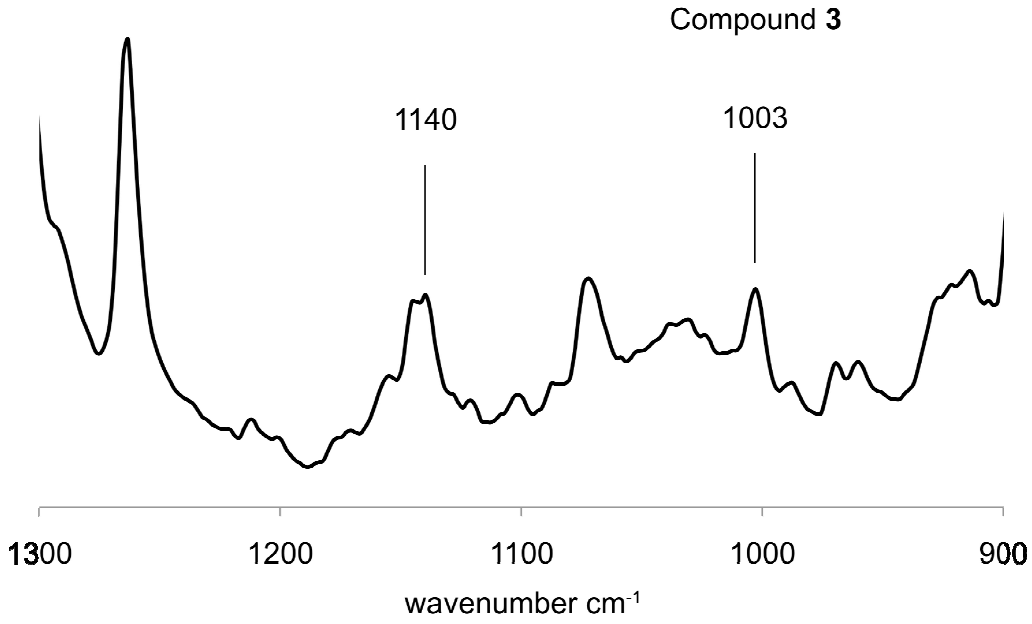

Figure S7. Solid state FTIR spectrum of **3**. Solvent was removed in vacuo from a methanolic solution of **3** prior to analysis. Labeled peaks are indicative of metal-sulfinate vibrations ($\nu_s(SO_2)$ = ~ 950 - 1050 cm^{-1}, $\nu_{as}(SO_2)$ = ~1100 - 1200 cm^{-1}.

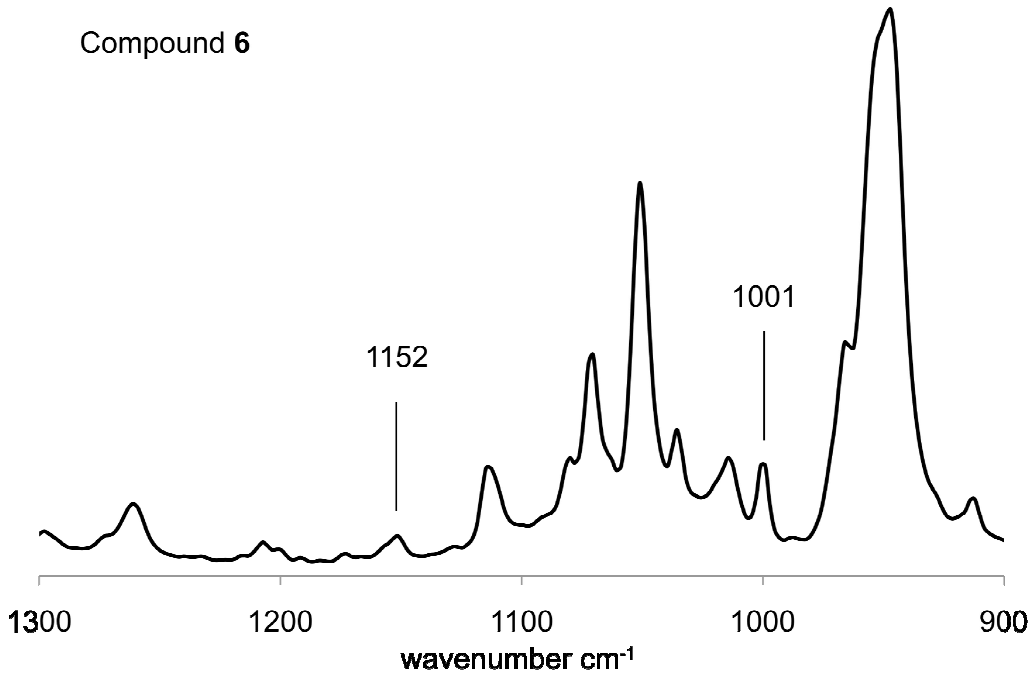

Figure S8. Solid state FTIR spectrum of compound **6**.. Labeled peaks are indicative of metal-sifinate vibrations ($\nu_s(SO_2)$ = ~ 950 - 1050 cm^{-1}, $\nu_{as}(SO_2)$ = ~1100 - 1200 cm^{-1}.

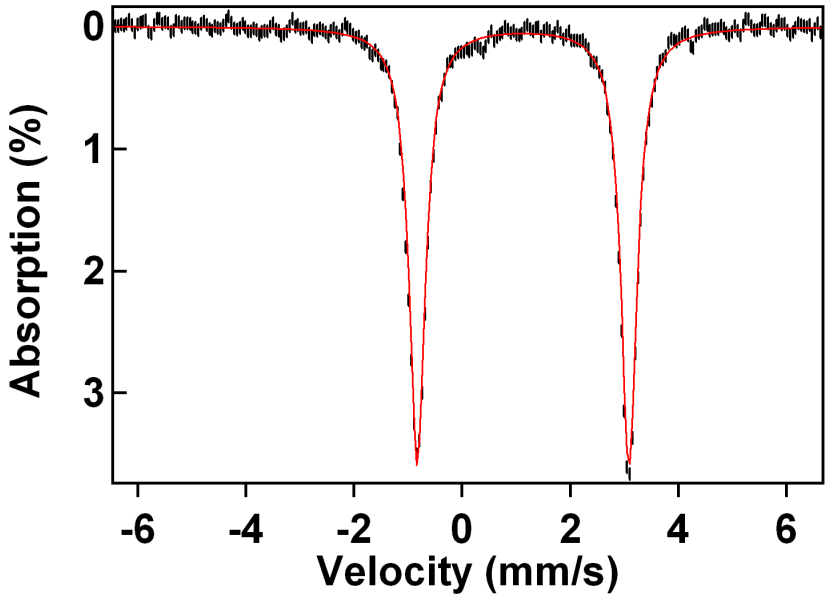

Figure S9. The 4.2-K Mössbauer spectra of **6** (solid sample, natural abundance iron in a nujol emulsion). Solid line is a spectral simulation of a doublet with ΔE_Q = 3.92 mm/s and δ = 1.13 mm/s.

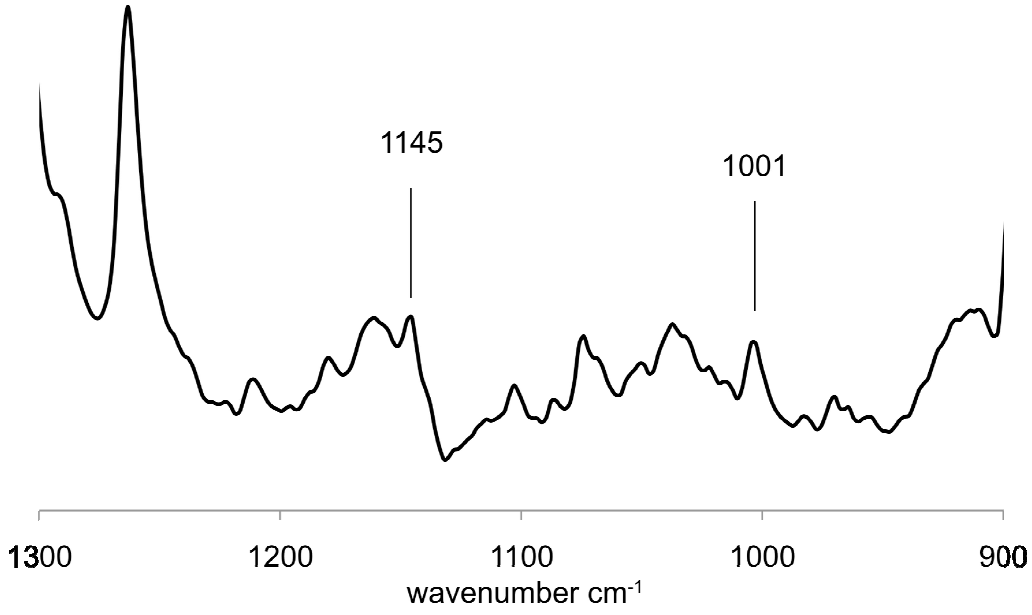

Figure S10. Solid state FTIR spectrum of the post-reaction mixture of the reaction between **7** and *m*-CPBA. Solvent was removed in vacuo prior to analysis. Labeled peaks are indicative of metal-sulfinate vibrations ($\nu_s(SO_2)$ = ~ 950 - 1050 cm^{-1}, $\nu_{as}(SO_2)$ = ~1100 - 1200 cm^{-1}.

Scheme S11. Extended Scheme 3. Postulated metal-mediated mechanism for the conversion of **1** to **3** in the reaction between **1** and *m*-CPBA without added base. Species in box are hypothesized intermediates.